University of Groningen

Size-Dependent Optical Properties of Dendronized Perylenediimide Nanoparticle Prepared by Laser Ablation in Water

Yasukuni, Ryohei; Sliwa, Michel; Hofkens, Johan; De Schryver, Frans C.; Herrmann, Andreas; Mullen, Klaus; Asahi, Tsuyoshi

IMPORTANT NOTE: You are advised to consult the publisher's version (publisher's PDF) if you wish to cite from it. Please check the document version below.

Document Version
Publisher's PDF, also known as Version of record

Link to publication in University of Groningen/UMCG research database

REGULAR PAPER

Size-Dependent Optical Properties of Dendronized Perylenediimide Nanoparticle Prepared by Laser Ablation in Water

Ryohei Yasukuni, Michel Sliwa[1], Johan Hofkens[2], Frans C. De Schryver[2], Andreas Herrmann[3], Klaus Müllen[4], and Tsuyoshi Asahi[*]

Department of Applied Physics, Osaka University, Suita, Osaka 565-0871, Japan
[1]*LASIR, UMR 8516, CNRS, Université des Sciences et Technologies de Lille, 59 655 Villeneuve d'Ascq Cedex, France*
[2]*Department of Chemistry and Center of Excellence in Catalysis (CECAT), Heverlee 3001, Belgium*
[3]*Department of Polymer Chemistry, Zernike Institute for Advanced Materials, University of Groningen, 9747 AG Groningen, The Netherlands*
[4]*Max-Planck-Institut für Polymerforschung, D-55128 Mainz, Germany*

Fluorescent nanoparticles of dendronized perylenediimide (DPDI) were fabricated by laser ablation in water. We succeeded in the preparation of colloidal nanoparticles of different sizes (150−400 nm) and examined their size-dependent optical absorption and fluorescence properties. The size-dependent extinction spectra can be explained by the effect of light scattering loss, and it was confirmed that their absorption spectrum is similar to that of molecules in solution. The very weak interchromophoric interaction is also confirmed by fluorescence spectral measurement. On the other hand, we found that the fluorescence quantum yield decreases with decreasing of the particle size, and we propose a new mechanism for the size-dependent reduction of emission intensity in organic nanoparticles. On the basis of the size dependent-fluorescence quantum yield and solvent polarity dependence of DPDI fluorescence in organic solvents, we considered that, while the interchromophoric interactions are weak in the nanoparticle, the excited singlet state migrates in a nanoparticle owing to energy hopping and is quenched at the surface, leading to the observed size-dependent fluorescence quantum yield (Φ_f) and a smaller value of Φ_f for nanoparticles than for the molecules in nonpolar solvents. © 2009 The Japan Society of Applied Physics

1. Introduction

Fluorescent organic compounds have attracted much attention because of their potential application as biological labels,[1,2] in light emitting diodes,[3] and as chemical sensors.[4] One recent and attractive research topic is the use of organic fluorescent compounds as a point light source in bioimaging[1,5] and microchip devices.[6] Indeed, recently, single molecule detection in combination with switchable fluorescent compounds and image reconstruction has enable a superspatial resolution (∼a few tens of nm) in fluorescence imaging, far beyond the optical diffraction limit.[7–9] Single-molecule fluorescence spectroscopy, however, is always confronted with the problem of limited photostability. Most commercial dyes undergo photobleaching in a few milliseconds under typical excitation conditions with a laser fluorescence microscope. In addition, the phenomenon of blinking, encountered in any single molecule system, interferes with the process under study. One idea for obtaining a stable point light source is to use an assembly of molecules in the form of a nanoparticle. Because large numbers of chromophores are incorporated, single nanoparticles show bright fluorescence even at a low excitation power, do not undergo rapid photobleaching, and give less emission blinking and off states that are generally observed in single-molecule experiments.[10]

Luminescent organic nanoparticles have been reported for several compounds;[11–13] however, the fabrication of highly fluorescent nanoparticles is generally not easy. In the solid state, molecules tend to aggregate and this leads to fluorescence quenching and/or excimer emission as a result of intermolecular interactions. For example, perylenediimide (PDI) is a well-known fluorescent dye with a high fluorescence quantum yield and a high photostability in solution. On the other hand, the emission spectrum of the
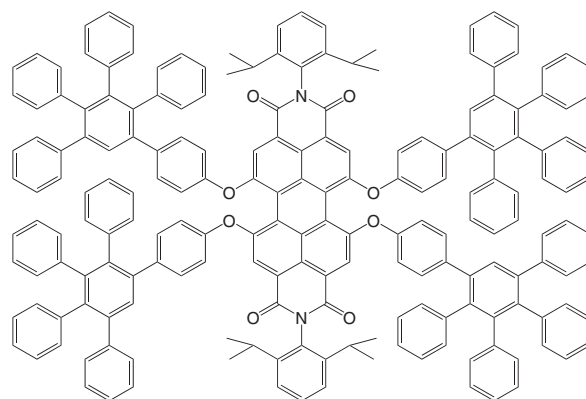

Fig. 1. The molecular structure of DPDI.

nanoparticles of commercially available PDIs shows characteristics of a strong intermolecular interaction (excimer-like emission) and a low fluorescence quantum yield.[14,15] Recently, we demonstrated the fabrication of highly fluorescent PDI nanoparticles by laser ablation in water using a bay-substituted dendronized PDI (DPDI, Fig. 1).[16] In DPDI, bulky dendron groups at the PDI chromophore bay positions hinder the electronic interactions among PDI chromophores. As a result, the fluorescence and absorption spectra of the nanoparticles are quite similar to those of DPDI molecules in solution. Furthermore, single-particle experiments on these laser-generated nanoparticles by time-correlated confocal fluorescence microscopy underline that the DPDI nanoparticles are bright and sufficiently photostable to be useful probes for single-particle fluorescence investigations.

In this study, we examine the size dependence of extinction and fluorescence properties of DPDI nanoparticle colloids prepared by laser ablation in water.[17–21] Colloidal nanoparticles with mean sizes ranging from 150 to 400 nm were successfully fabricated by varying the laser fluence.

[*]E-mail address: asahi@ap.eng.osaka-u.ac.jp

The shape and the maximum band wavelength of the extinction spectra depending on the particle size are discussed on the basis of Mie theory by comparing the extinction spectra to numerical simulations. We also found that the fluorescence quantum yield was influenced strongly by the particle size and/or laser fluence although the spectral shape was not. The yield decreased about a seventh as the size decreased from 400 to 150 nm. In our previous paper, it was suggested that nonradiative deactivation of the excited state is enhanced in the nanoparticles compared with DPDI molecules in solution and that fluorescence quenching at the particle surface or impurities should be considered.[16] We examine herein the particle size dependence and the effect of laser irradiation on the fluorescence intensity and present a rationale that involves fluorescence quenching at the surface of the nanoparticles in water.

2. Experimental Procedure

The synthesis of DPDI has been described previously,[22] and its colloidal nanoparticles have been prepared by the laser ablation method.[15–20] In brief, DPDI powder was put in an aqueous solution of 8 mM 3-[(3-cholamidopropyl)dimethyl-ammonio]propanesulfonate (CHAPS; Dojin). Next, the suspension (3×10^{-3} wt %) was sonicated for 30 min. The mixture (3.0 mL) was put in a $1 \times 1 \times 5$ cm³, quartz cuvette, stirred vigorously with a magnetic stirrer, and then exposed to the frequency-doubled beam of a nanosecond YAG laser (Continuum Surelite II, 532 nm, 10 Hz, 8 ns full width at half maximum). The spot area was approximately 22 mm², and the laser intensity was adjusted using a polarizer.

The ultraviolet–visible (UV–vis) extinction and emission spectra of the nanoparticle colloidal solution were measured with a UV–vis–near infrared (NIR) scanning spectropho-tometer (Shimadzu UV-3100PC) and a fluorescence spec-trophotometer (Hitachi F-4500), respectively. The size of nanoparticles was estimated by dynamic light scattering (DLS) measurements (Malvern Instruments Zetasizer), and their zeta potential was also evaluated using the same equipment. The morphology of the prepared nanoparticles was observed using a scanning electron microscope (SEM; FEI Strata DB235-31).

3. Results and Discussion

3.1 Nanoparticle formation by laser ablation

The initial sample powder, when mixed in water, sinks to the bottom of the cuvette and its supernatant is almost colorless. This indicates that DPDI hardly dissolves in water, as can be expected form its hydrophobic character. When the suspen-sion is exposed to laser pulses at laser fluences above the threshold, it is gradually transformed to a magenta trans-parent colloidal solution. The apparent absorption spectra of the supernatants obtained after letting the solution settle for 1 h are shown in Fig. 2(a). The spectra at laser fluences above 40 mJ/cm² show similar features as the spectra of solutions of DPDI molecules. In addition, long wavelength tails are observed owing to light scattering. These spectral features are characteristic of the nanoparticle colloidal solutions.

The absorbance at 570 nm is plotted as a function of the laser fluence in Fig. 2(b). The absorbance increases when the laser fluence is above the threshold of 40 mJ/cm² and saturates for fluences higher than 180 mJ/cm². The depend-
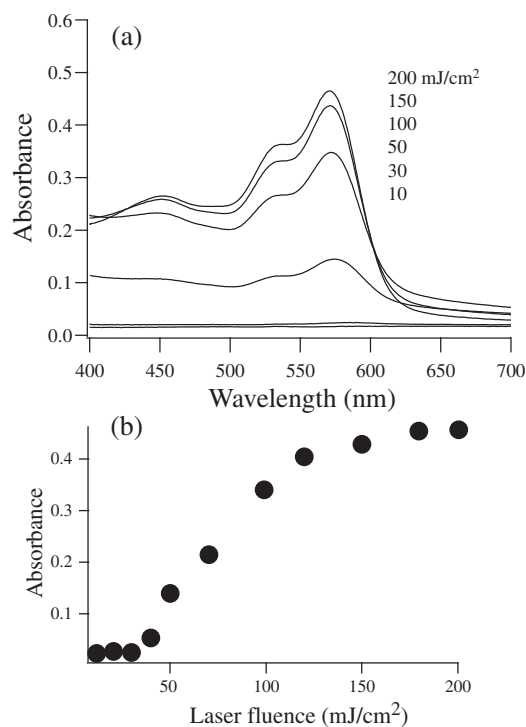
Fig. 2. (a) Laser fluence dependence of absorption spectra of DPDI water suspensionsafter 10 min laser irradiation. The laser fluence is given in the figure. (b) The peak absorbance of a DPDI water suspension after 10 min laser irradiation as a function of laser fluence.
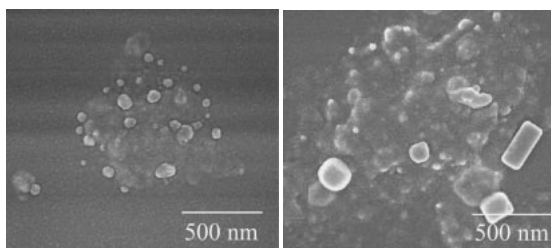
ence on fluence demonstrates clearly that the nanoparticle formation requires high photon density, similar to the case of laser ablation-induced nanoparticle formation by other organic dyes in water.[17–22] At higher laser fluences, the colloidal solution of DPDI nanoparticles is stable and the absorption spectrum does not change significantly even after the solution is settled for a week at room temperature. To verify molecular decomposition by the intense laser light, the water in the colloidal solution was allowed to evaporate in a vacuum chamber. The material left was dissolved again in ethanol, and the absorption spectrum of the ethanol solution was measured. The shape of the spectrum of the colloidal solution in ethanol corresponds closely to that of DPDI molecules in an ethanol solution in the wavelength region from 250 to 800 nm. No additional absorption bands are observed. From these data, it can be concluded that molecular decomposition can be neglected under the laser excitation conditions used.

We prepared nanoparticle colloids by laser irradiation at 50, 100, 150, and 200 mJ/cm² for 10 min, followed by centrifugation at 3000 rpm for 10 min to remove micro-meter-sized crystals. DLS measurements of the obtained nanoparticle colloids (see Table I) demonstrated that mean particle sizes and the polydispersity indexes (pdi) decreased with increasing laser fluence. To characterize nanoparticles directly, we measured SEM images of nanoparticles at 200 mJ/cm² laser fluence. To remove the maximum amount of surfactant from the colloidal solution, the colloidal solution was centrifuged at 15000 rpm for 30 min, the colorless supernatant was replaced by pure water, and then the nanoparticle redispersed by sonication. A drop of the nanoparticle dispersion was spread on a surface-modified

Table I. Mean particles size (*d*), absorption maximum wavelength (λ_{max}), and fluorescence quantum yield (Φ_f) of DPDI nanoparticle colloidal solutions and those of DPDI solutions in acetone and toluene.

Laser fluence (mJ/cm²)	*d* (nm)/(pdi)	λ_{max} (nm)	Relative fluorescence intensity[a]	Φ_f[b]
50	436/(0.299)	577	0.055	0.13
100	261/(0.229)	573	0.038	0.055
150	177/(0.207)	571	0.023	0.027
200	156/(0.103)	571	0.019	0.018
Acetone	—	573	0.19	0.17
Toluene	—	581	1	0.92

a) Relative fluorescence intensities of the colloidal and molecular solutions normalized with respect to the toluene solution; optical density of each sample is 0.05 at the excitation wavelength (570 nm).

b) Fluorescence quantum yields using the DPDI toluene solution as a reference. ($\Phi_f = 0.92$).[22]

Fig. 4. Normalized extinction spectra of DPDI colloidal nanoparticles prepared at different fluence and the absorption spectrum of a DPDI acetone solution. The laser fluence is given in the figure.


Fig. 3. SEM image of DPDI nanoparticles. Nanoparticles are observed together with surfactant deposited from the solution.

silicon substrate and dried in a vacuum chamber. After coating its surface with a thin gold layer (5 nm thick), SEM images were recorded. Figure 3 shows two selected pictures. First of all, despite centrifugation to remove the surfactant, a considerable amount of the surfactant remained on the sample. Its aggregation is characterized by the cloud-like gray background on the SEM images which render the small-sized particles difficult to distinguish. On the other hand, we clearly see sharp-edged structures like the cubic or rectangular ones (with a size from 100 to 300 nm) which can be considered to be DPDI nanoparticles. Using such discrimination, we can observe nanoparticles with sizes between 50 to 300 nm. Even if the SEM images allow us to see DPDI particles, however, the size characterization is not fruitful in this case due to surfactant aggregation.

3.2 Size dependence of extinction spectrum

In the preceding section, we described that the mean size of the prepared nanoparticles can be changed by varying the laser fluence. Here, we discuss the size dependence of their optical properties in detail. The absorption spectra of colloidal solutions prepared at different fluences are shown in Fig. 4. Each spectrum was normalized at the maximum band wavelength. The spectra show a gradual tail in the region wavelength longer than 620 nm where the molecule in solution has no absorption, and the peak position shifts to longer wavelengths with increasing particle size. It is worth noting that conventional absorption measurements of colloid samples provide an optical extinction that is the sum of optical absorption and scattering coefficients. The extinction coefficient α_{ext} is given by absorption σ_{abs} and scattering σ_{sca} cross sections, and the number of particles, *N*, as follows:
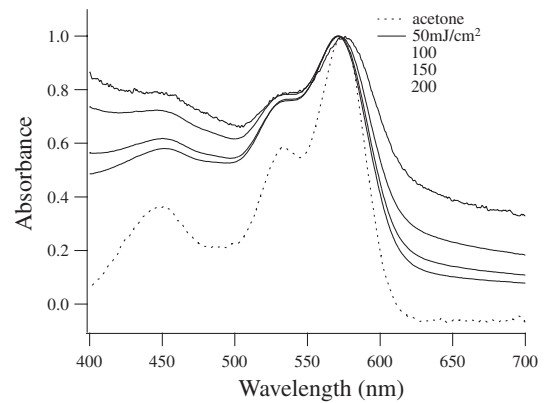
$$\alpha_{ext} = N(\sigma_{abs} + \sigma_{sct}). \quad (1)$$

The relative contribution of the two components in the extinction is a function of the particle size, and scattering becomes dominant in larger-sized nanoparticles. Therefore, the spectral measurement of extinction does not give direct information on the size-dependent maximum position of the optical absorption band.

In order to explain the size-dependent extinction spectra, we calculated the extinction, scattering, and absorption coefficient of spherical DPDI nanoparticles having the complex refractive index of the nanoparticle given in Fig. 5(a) on the basis of Mie theory using the algorithm described in ref. 23. We estimated the imaginary part of the complex refractive index κ from the absorption spectrum of a DPDI acetone solution as

$$\kappa = \frac{\lambda}{4\pi} \varepsilon c. \quad (2)$$

Here, ε and *c* are the molar absorption coefficient in solution and the concentration of DPDI molecules in a nanoparticle, respectively. Because electronic interactions between PDI chromophore are very weak due to the bulky dendron groups in the bay positions, we can safely assume that the absorption spectra of DPDI in both solid state and solution are virtually the same. We set the molar concentration of the nanoparticle to be 0.58 mol/dm³. On the other hand, the real part, *n*, was calculated by the Kramers–Kronig relation given by

$$n(\lambda) = \int_0^\infty \frac{\kappa(\lambda)}{\lambda[1 - (\lambda/\lambda')^2]} \, d\lambda + n_0, \quad (3)$$

where n_0 is the refractive index at a wavelength far from the resonance absorption band, and here it was assumed to be 1.6.

The calculated extinction, scattering, and absorption cross sections for spherical nanoparticles having different diameters are shown in Figs. 5(b)–5(d), where all spectra are normalized by the value at the maximum. The simulated extinction spectra show the same features of size dependence as the experimental ones. The maximum band wavelength shifts from 592 to 581 nm as the size of the nanoparticles decreases from 500 to 100 nm. The simulation indicates that the gradual tail of the extinction in the longer
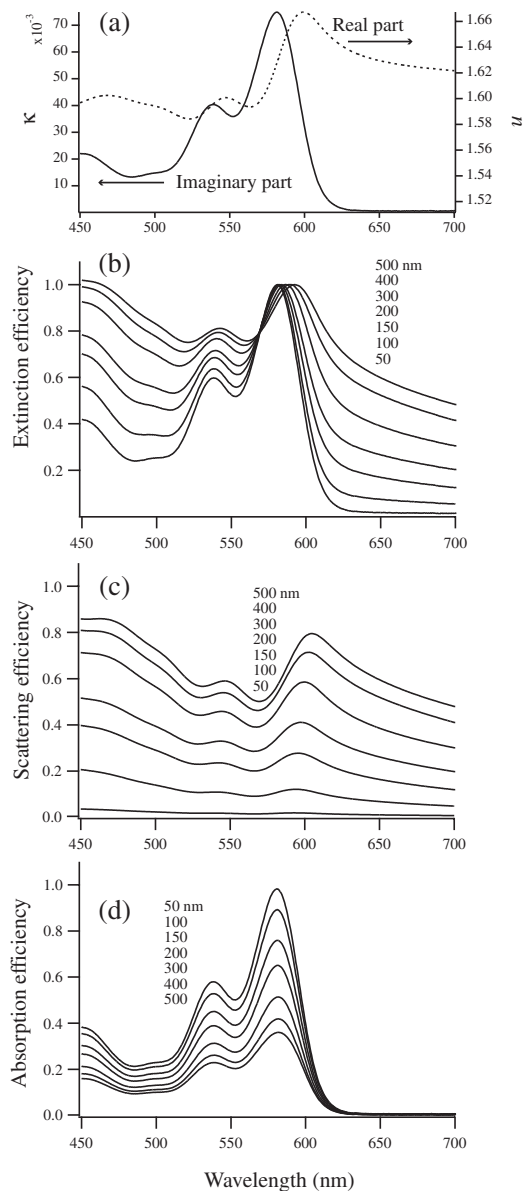
Fig. 5. Simulation using Mie theory for various sized DPDI spherical nanoparticles: (a) complex refractive index ($n + i\kappa$) of DPDI in the solid state, (b) extinction, (c) scattering, and (d) absorption efficiency. Mean particle sizes are given in the figure.

wavelength region is due to light scattering, and that the scattering contribution increases with particle size, while the absorption spectrum is independent of particle size. Therefore, it can be concluded that the scattering loss is the main reason for the size dependence of the extinction spectra and for the discrepancy in the spectra between the colloidal nanoparticle solutions and the solutions of DPDI.

It should be noted here that in many reports of the size dependence of the optical extinction of organic nanoparticles, the size-dependent absorption was discussed mainly from the viewpoint of the geometrical effect of molecular packing in nanoparticles that results in changes of electronic interactions between molecules in a bulk crystal. In the case of DPDI, on the other hand, the absorption spectrum is not sensitive to the manner of molecular packing because of a very weak electronic interaction between chromophores due to bulky dendron groups, so we can elucidate the details of the effect of light scattering loss in the extinction spectra.
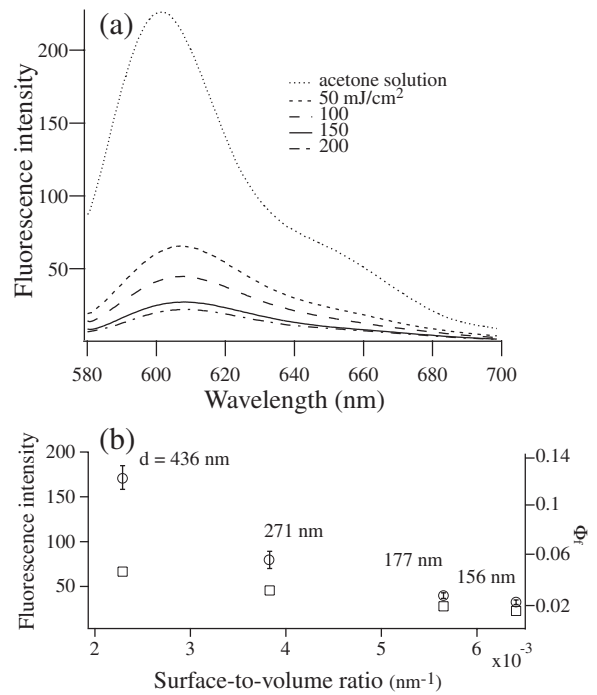
Fig. 6. (a) The emission spectra of DPDI nanoparticle colloids prepared by 532 nm nanosecond laser irradiation at fluences of 50, 100, 150, and 200 mJ/cm^2 for 10 min, and the spectrum of a 2 μM acetone solution. The excitation wavelength for emission measurements was 570 nm. (b) Emission intensities of different-sized DPDI nanoparticle colloids as a function of the surface-to-volume ratio (○), and the fluorescence quantum yields estimated by taking into account the scattering loss of the excitation light (□). Mean particle size is given in the figure.

Indeed, in this work we have demonstrated clearly that the scattering effect is important to consider when interpreting the size dependent extinction spectrum of nanoparticle colloids, and the experimental observation can be explained semi qualitatively on the basis of Mie scattering theory in the case of DPDI.

3.3 Size dependence of fluorescent properties

In Fig. 6(a), we present the fluorescence spectra of DPDI colloidal solutions obtained at several laser fluences along with the spectrum of a DPDI acetone solution. Optical densities (i.e., extinction) at the excitation wavelength (570 nm) were set to the same value (0.05). The relative fluorescence intensities of the nanoparticle colloidal solution and the acetone and toluene solutions are shown in Table I. The shape of the fluorescence spectra of the nanoparticle colloids obtained at different fluences are nearly identical and similar to the spectrum recorded for the DPDI acetone solution. A very weak interchromophoric interaction is also confirmed by the similarities in the fluorescence spectra. On the other hand, the fluorescence yield of the colloidal solutions depends on the particle size, and it is lower than that of the acetone solution.

We estimated the fluorescence quantum yield of the nanoparticles using a DPID toluene solution as the reference ($\Phi_f = 0.92$)[22] and by considering the influence of the scattering loss of the excitation light in the fluorescence measurement. Indeed, as described previously, the optical density of a colloidal sample does not equal its optical

absorption. Using the numerically simulated spectra in Fig. 5, we can calculate the "true" optical absorption of DPDI nanoparticles for each colloidal sample. For example, in the case of a 300 nm nanoparticle colloid, the true absorption is about 50% of its optical density obtained by a conventional absorption measurement. Taking into account the light scattering loss as outlined, we evaluated Φ_f for the colloidal nanoparticles of different size. The values are listed in Table I together with those of acetone and toluene solutions of DPDI.

In our previous paper, we reported that Φ_f of 300 nm nanoparticles was about 0.6, by assuming Φ_f of the acetone solution to be one.[16] However, this assumption was wrong. We measured Φ_f for an acetone solution and obtained a value of 0.17, which is smaller than the values obtained for methylcyclohexane (0.96), toluene (0.92), and tetrahydrofuran (THF) (0.77) solutions.[22] This result indicates that Φ_f of DPDI molecules depends on the solvent polarity: methylcyclohexane, $\varepsilon = 2.02$; toluene $\varepsilon = 2.38$; THF, $\varepsilon = 7.58$; acetone, $\varepsilon = 21$. In a previous paper, we have already shown that electron donor groups on the side bay of the PDI can increase nonradiative decay especially in a polar medium;[24] therefore, the dendron group at the side bay of the PDI core can act as an electron donor. Intramolecular electron transfer induced by photoexciting the PDI core may take place in a highly polar solvent such as acetone, resulting in a reduced Φ_f.

The smaller value of Φ_f of the nanoparticle colloids than that of molecules in solution means that non-radiative deactivation channels exist for excited states in the nanoparticles. As mentioned in §1, reduction of emission intensity in nanoparticles was observed and discussed for commercially available PDIs, and the reduction was attributed to a strong electronic interaction between molecules (chromophores) leading to excimer formation with a low fluorescence quantum yield and to enhancement of nonradiative transition rates.[14,15] However, such a consideration is not probable for DPDI nanoparticles because interchromophoric interaction is very weak. Consequently, we consider here fluorescence quenching at the surface of the nanoparticle and discuss the size-dependent reduction of the fluorescence quantum yield. As shown in Fig. 6(b), the value of Φ_f becomes lower for smaller nanoparticles and correlates well to the surface-to-volume ratio of the nanoparticle, estimated by assuming spherical particles. The result indicates that fluorescence quenching can be linked to the surface of the nanoparticles. We considered that surface molecules play an important role as fluorescence quenching sites, because the Φ_f of DPDI molecules decreases markedly in highly polar solvents. As DPDI molecules in the nanoparticle located at the particle surface are surrounded by water ($\varepsilon = 80.4$), their Φ_f is much lower compared with molecules inside the nanoparticle. The latter molecules indeed 'feel' an apolar environment comparable to nonpolar solvents. Moreover, the excited states can migrate between several molecules during an intrinsic lifetime in a nanoparticle by Förster energy transfer. Indeed, the considerably large overlap of absorption and emission spectra of DPDI result in efficient energy hopping.[24] Therefore, some of the excited states reach the surface and, as a consequence, they are quenched.[25] As the probability of surface quenching
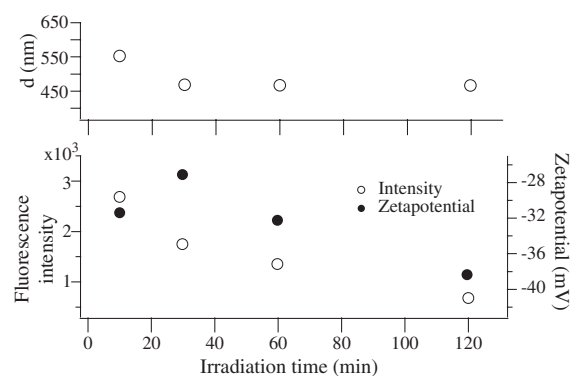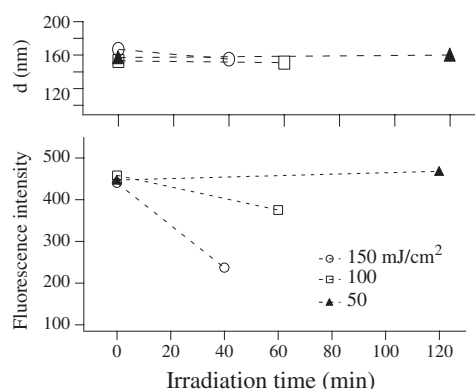

Fig. 7. Mean particle size (*d*, top), fluorescence intensity (○), and zeta potential (●, bottom) of a DPDI nanoparticle colloidal solution after laser irradiation at 50 mJ/cm^2 as a function of laser irradiation time.

increases with decreasing particle size, the fluorescence intensity becomes weaker for smaller nanoparticles. The small value of $\Phi_f = 0.018$ for nanoparticles with a mean diameter of 150 nm indicates efficient migration of the excited singlet state in the nanoparticles. When assuming that Φ_f of DPDI molecules inside nanoparticles is almost unity and that at the surface zero, we consider that 90% of the excited singlet states generated in a nanoparticle migrate to the surface and are quenched, which suggests the diffusion length of the excited state to be on the order of 100 nm.

In the laser-assisted colloid preparation method that was used here, particle size is varied by changing laser fluence. The intense pulse laser irradiation likely generates fluorescence quenching sites or species in the nanoparticles. To examine the laser irradiation effect on the fluorescence intensity, we measured the dependence of the fluorescence intensity on irradiation time, the particle size, and the zetapotential at a fixed laser fluence of 50 mJ/cm^2. The results are shown in Fig. 7. In the first 30 min of irradiation, both the fluorescence intensity and the size decrease with irradiation time. This agrees with the particle size dependence shown in Fig. 6(b). After this point (30 min), further increasing the irradiation time does not result in any further change in the particle size. In contrast, the fluorescence decreases continuously, and also the zetapotential of the colloid become smaller with increasing irradiation time. Since a change of the zetapotential can be interpreted as the formation of charged species at the particle surface, it is likely that laser-induced ionization or oxidization of molecules occurs at the surface, which would partially contribute to the fluorescence quenching.

We also examined the fluorescence intensity of nanoparticle colloids prepared by 200 mJ/cm^2 laser irradiation for 10 min followed by further laser excitation under different irradiation conditions (50 mJ/cm^2 for 120 min, 100 mJ/cm^2 for 60 min, and 150 mJ/cm^2 for 40 min). Note that the total number of irradiated photons is the same in all excitation conditions but they are delivered differently to the nanoparticles. Although the particle size did not change when the second part of the laser irradiation was applied in sequence, the fluorescence intensity decreased at laser fluences of 100 and 150 mJ/cm^2 but not at the fluence of

Fig. 8. The dependence of mean particle size (*d*, top) and fluorescence intensity (bottom) on laser fluence and time on the sequence of laser irradiation to the DPDI nanoparticle colloidal solution prepared at 200 mJ/cm^2 laser irradiation for 10 min. Irradiated laser fluences are 150 (○), 100 (□), and 50 (▲) mJ/cm^2.

50 mJ/cm^2 (Fig. 8). These results suggest that higher fluences generate more fluorescence quenching sites in the nanoparticle prepared at 200 mJ/cm^2.

At the current stage of this work, it is clear that the solvent plays a strong role in the fluorescence quenching of nanoparticles but the exact mechanism of the size-dependent fluorescence yield has not yet been established. Fluorescence decay measurements in a single particle and in different environments seem to be indispensable for investigating the excited state dynamics and fluorescence quenching mechanism in more detail. Moreover, influence of the surfactant should be taken in account as we demonstrated that the quenching mechanism happens essentially at the surface which is surrounded by surfactant. We are currently conducting such experiments.

4. Conclusions

DPDI nanoparticle colloids of different sizes were prepared by laser ablation in water, and the size dependence of their optical properties was characterized. We attribute the size-dependent extinction spectra to light scattering loss, which becomes dominant for large particles. Both the absorption and the emission spectra are similar to those of molecules in solution, which indicated weak electronic interactions bwtewwn the PDI moieties owing to the bulky dendron groups situated in the bay positions of the PDI core. We found that the fluorescence intensity depends on the particle size and that it is smaller than that of DPDI molecules in nonpolar solvents. While the interchromophoric interactions are weak in the nanoparticles, the excited singlet state can migrate through the nanoparticle by energy hopping and can be quenched at the surface, leading to the observed size-dependent fluorescence quantum yield. Because the surface molecules of the nanoparticle in water feel a polar environment, their fluorescence yield is reduced, probably due to intramolecular electron transfer from the dendrons to the core. Therefore, the surface molecules act as fluorescence quenching sites. The laser irradiation effect on the fluorescence intensity suggests that ions or oxidized species are generated at the particle surface under the intense laser excitation used. This further contributes to fluorescence quenching at the surface.

1) R. Kraayenhof, A. J. W. G. Visser, and H. C. Gerritsen: *Fluorescence Spectroscopy: Imaging and Probes* (Springer, Tokyo, 2002) p. 297.
2) A. Waggoner: Curr. Opin. Chem. Biol. **10** (2006) 62.
3) R. Jagannathan, G. Irvin, T. Blanton, and S. Jagannathan: Adv. Funct. Mater. **16** (2006) 747.
4) B. Schazmann, N. Alhashimy, and D. Diamond: J. Am. Chem. Soc. **128** (2006) 8607.
5) I. Koyama-Honda, K. Ritchie, T. Fujiwara, R. Iino, H. Murakoshi, R. S. Kasai, and A. Kusumi: Biophys. J. **88** (2005) 2126.
6) H. J. Kim, J. Lee, T. H. Kim, T. S. Lee, and J. Kim: Adv. Mater. **20** (2008) 1117.
7) K. I. Willing, S. O. Rizzoli, V. Westphal, R. Jahn, and S. W. Hell: Nature **440** (2006) 935.
8) P. Dedecker, J. Hotta, C. Flors, M. Sliwa, H. Ujii, M. B. J. Roeffaers, R. Ando, H. Mizuno, A. Miyawaki, and J. Hofkens: J. Am. Chem. Soc. **129** (2007) 16132.
9) C. Flors, J. Hotta, H. Uji-i, P. Dedecker, R. Ando, H. Mizuno, A. Miyawaki, and J. Hofkens: J. Am. Chem. Soc. **129** (2007) 13970.
10) J. N. Clifford, T. D. M. Bell, P. Tinnefeld, M. Heilemann, S. M. Melnikov, J. Hotta, M. Sliwa, P. Dedecker, M. Sauer, J. Hofkens, and E. K. L. Yeow: J. Phys. Chem. B **111** (2007) 6987.
11) S. Li, L. He, F. Xiong, Y. Li, and G. Yang: J. Phys. Chem. B **108** (2004) 10887.
12) F. Debuigne, L. Jeunieau, M. Wiame, and J. B. Nagy: Langmuir **16** (2000) 7605.
13) Y.-Y. Sun, J.-H. Liao, J.-M. Fang, P.-T. Chou, C.-H. Shen, C.-W. Hsu, and L.-C. Chen: Org. Lett. **8** (2006) 3713.
14) J. Gesquiere, T. Uwada, T. Asahi, H. Masuhara, and P. F. Barbara: Nano Lett. **5** (2005) 1321.
15) S. Masuo, A. Masuhara, T. Akashi, M. Muranushi, S. Machida, H. Kasai, H. Nakanishi, H. Oikawa, and A. Itaya: Jpn. J. Appl. Phys. **46** (2007) L268.
16) R. Yasukuni, T. Asahi, T. Sugiyama, H. Masuhara, M. Sliwa, J. Hofkens, F. C. De Schryver, M. Van der Auweraer, A. Herrmann, and K. Müllen: Appl. Phys. A **93** (2008) 5.
17) T. Asahi, T. Sugiyama, and H. Masuhara: Acc. Chem. Res. **41** (2008) 1790, and references therein.
18) T. Sugiyama, T. Asahi, and H. Masuhara: Chem. Lett. **33** (2004) 724.
19) Y. Tamaki, T. Asahi, and H. Masuhara: J. Phys. Chem. A **106** (2002) 2135.
20) T. Sugiyma, T. Asahi, H. Takeuchi, and H. Masuhara: Jpn. J. Appl. Phys. **45** (2006) 384.
21) H.-G. Jeon, T. Sugiyama, H. Masuhara, and T. Asahi: J. Phys. Chem. C **111** (2007) 14658.
22) J. Qu, N. G. Pschirer, D. Liu, A. Stefan, F. C. De Schryver, and K. Müllen: Chem.—Eur. J. **10** (2004) 528.
23) C. F. Bohren and D. R. Huffman: *Absorption and Scattering of Light by Small Particles* (Wiley, New York, 1983).
24) C. Flors, I. Oesterling, T. Schnitzler, E. Fron, G. Schweitzer, M. Sliwa, A. Herrmann, M. Van der Auweraer, F. C. De Schryver, K. Müllen, and J. Hokens: J. Phys. Chem. C **111** (2007) 4861.
25) E. Botzung-Appert, V. Monnier, T. Ha Duong, R. Pansu, and A. Ibanez: Chem. Mater. **16** (2004) 1609.